Sandwich-Type N-C@$CoTe_2$@C Anode: A Stress-Buffer Nanostructure for Stable Sodium-Ion Storage

Lixiang Wang,*[a] Yahua Hu,[a] Khak Ho Lim,[c] Wei Zhang*[b]

[a] School of Mechanical and Electrical Engineering, Jiaxing Nanhu University, Zhejiang, 314001, China. Email: wlx@jxnhu.edu.cn

[b] School of Materials and Energy, Guangzhou Key Laboratory of Low-Dimensional Materials and Energy Storage Devices, Guangdong University of Technology, Guangzhou, 510006, China. Email: zhwei@gdut.edu.cn

[c] Institute of Zhejiang University-Quzhou, Zhejiang, 324000, China.

Section I. Supporting information of calculation details

1. Calculation process of the carbon content in N-C@$CoTe_2$@C from TG result

The content of carbon in in N-C@$CoTe_2$@C composite was measured by the final solid product is $Co_2Te_3O_8$ after TGA test.

$C(s) + O_2(g) \rightarrow CO_2(g)$

$2CoTe_2(s) + 4O_2(g) \rightarrow Te(g) + Co_2Te_3O_8(s)$

Therefore, the weight percentage of carbon could be calculated by the following formula:

$$1 - (Co_2Te_3O_8\% \times \frac{M_{Co_2Te_3O_8}}{2M_{CoTe_2}}) = 1 - (1.16 \times Co_2Te_3O_8\%) = 49.75\%$$

Where $M_{Co2Te3O8}$ and M_{CoTe2} are the molecular mass of $Co_2Te_3O_8$ and $CoTe_2$, respectively. The total $CoTe_2$ content in N-C@$CoTe_2$@C composite is calculated to be ~50.75 wt%.

2. Calculation process of the capacitance effect and pseudocapacitive contribution

The capacitance effect can be determined from the CV curves at various scan rates according to the relationship between measured peak currents (i), and scanning rates (v), as follows:

$$i = a\, v^b$$

$$\log i = b \log v + \log a$$

where a and b are the fitting parameters, i and v represent peak current and scanning rate, respectively. The value of variable parameter b is deduced by the slope of log (i)/log (v) with a range of 0.5–1.0. The electrochemical reaction is controlled by ion diffusion if the b approaches 0.5. While the value nearing 1.0 means that the electrochemical reaction is dominated by capacitive behavior.[1, 2]

Furthermore, the pseudocapacitive contribution at various scan rates could be quantitatively calculated via the following equation:

$$i = k_1 v + k_2 v^{1/2}$$

where $k_1 v$ and $k_2 v^{1/2}$ represent the contribution of the capacitive and diffusion behaviors, respectively.

3. Calculation process of the diffusion coefficient (D_{Na+})

The galvanostatic intermittent titration technique (GITT) tests were performed by discharging or charging the cells for 30 min at 50 mA g^{-1} followed by a 30 min relaxation in the voltage range of 0.01 to 3.0 V. The D_{Na^+} value could be calculated based on the equation:

$$D_{Na^+} = \frac{4}{\pi t}\left(\frac{V_m m_B}{S M_B}\right)^2 \left(\frac{\triangle E_s}{\triangle E_t}\right)^2 \left(t \ll \frac{L^2}{D}\right)$$

where t is the duration of the current impulse (s), S is the area of the electrode (cm^2), m_B (g), M_B (g mol^{-1}) and V_m (cm^3 mol^{-1}) are the mass, the molar mass, and the molar volume of the active material, respectively. ΔE_s and ΔE_t represent the difference of two adjacent steady state voltages and the difference of voltage before and after constant current pulse, respectively. [3, 4]

Section II. Supplementary Figures and Tables

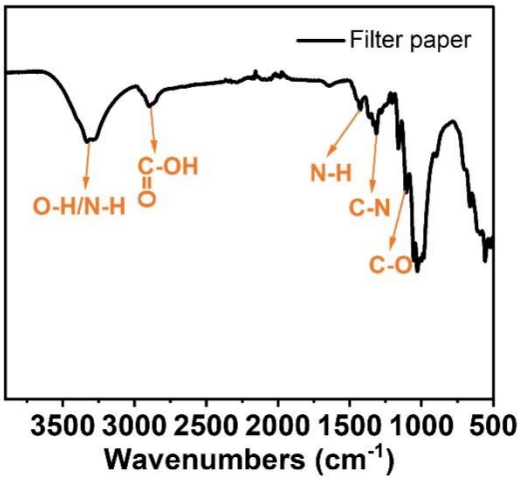

Figure S1. FTIR spectrum of filter paper from 500 to 3800 wavenumbers.

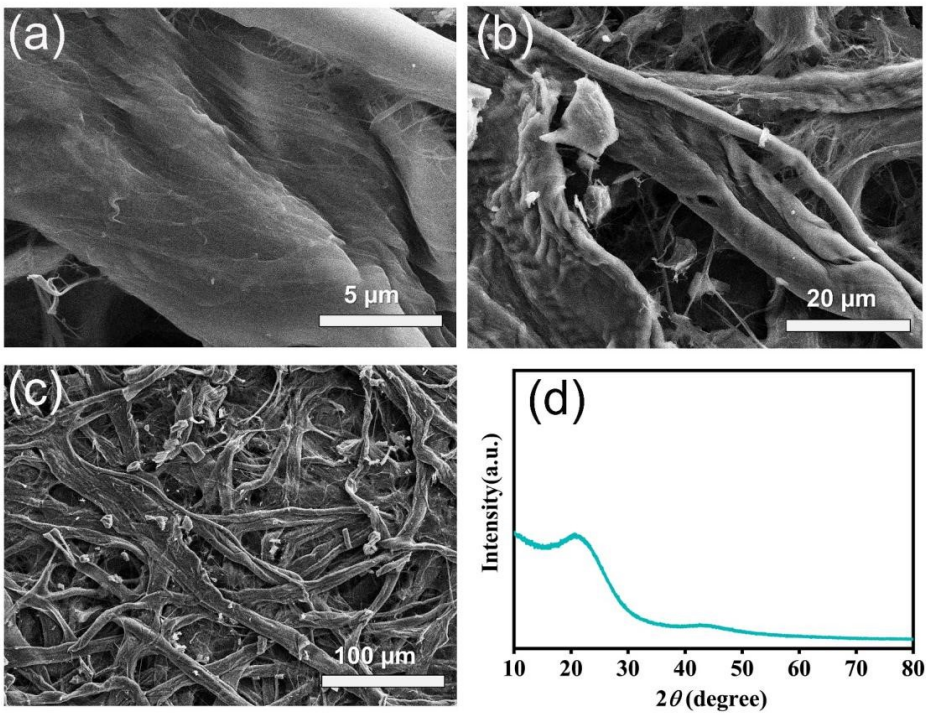

Figure S2. SEM figures and XRD pattern of pure C fibers.

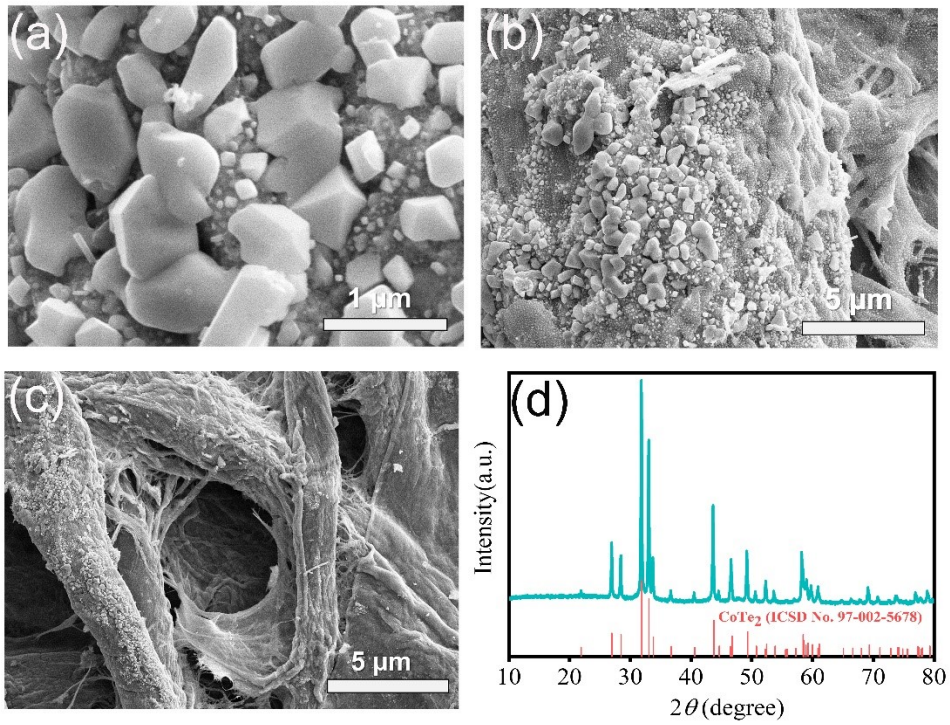

Figure S3. SEM figures (a-c) and XRD pattern (d) of $CoTe_2$@C composite.

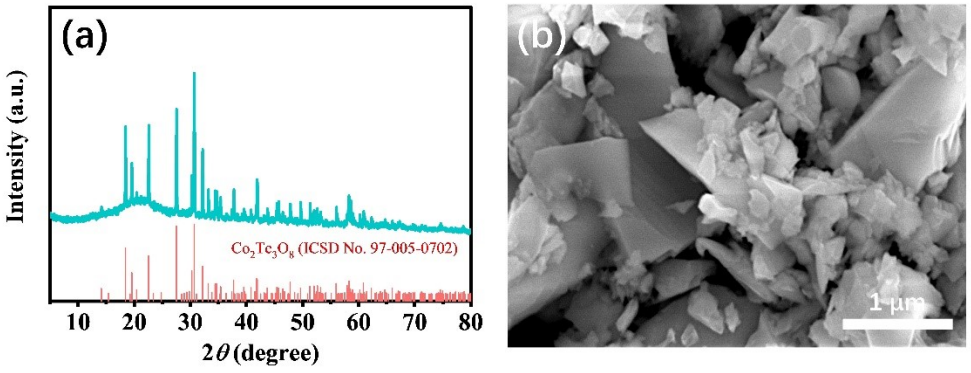

Figure S4. SEM image (a) and XRD pattern (b) of the N-C@$CoTe_2$@C residue after TGA analysis. It is obvious that N-C@$CoTe_2$@C was fully oxidized into $Co_2Te_3O_8$ after TGA analysis.

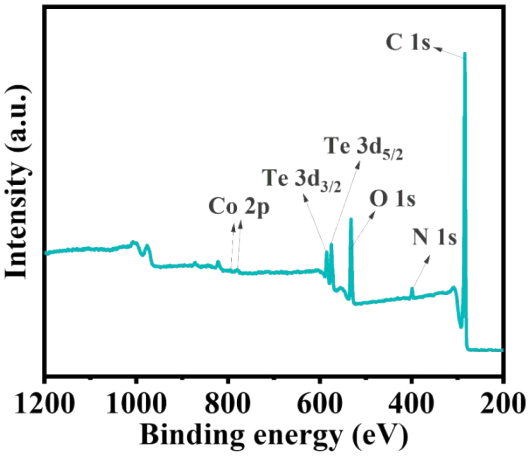

Figure S5. XPS survey spectrum of N-C@$CoTe_2$@C composite.

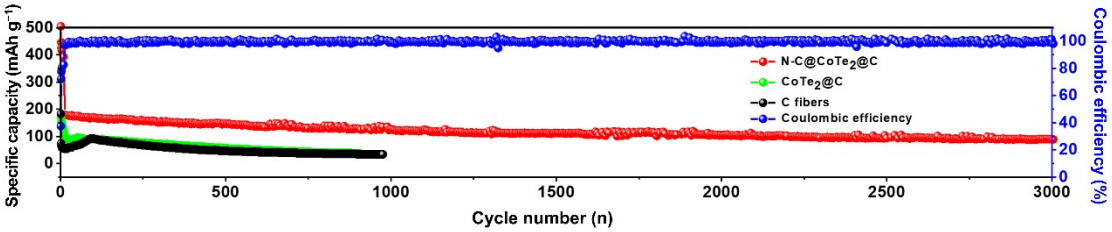

Figure S6. Cyclic stability of the N-C@$CoTe_2$@C composite at 1 A g^{-1}.

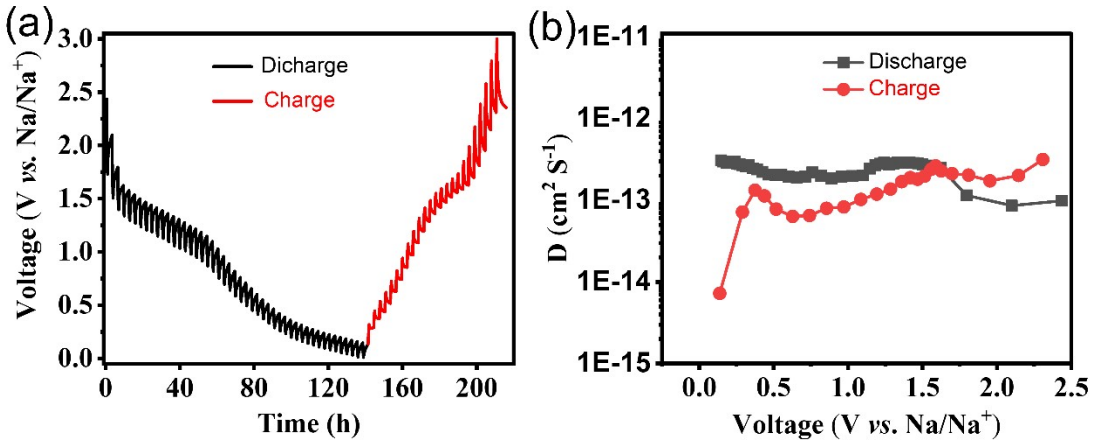

Figure S7. GITT curves and corresponding D_{Na^+} values of $CoTe_2$@C electrode.

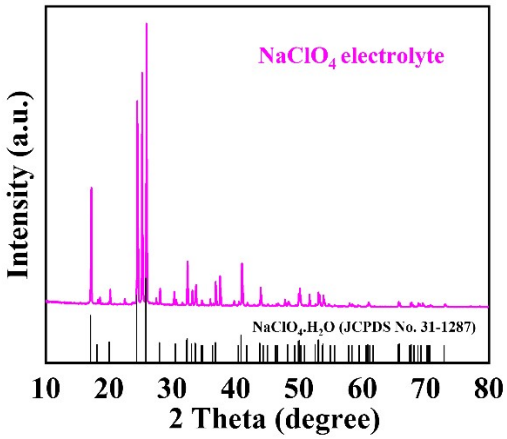

Figure S8. XRD pattern of the $NaClO_4$ electrolyte.

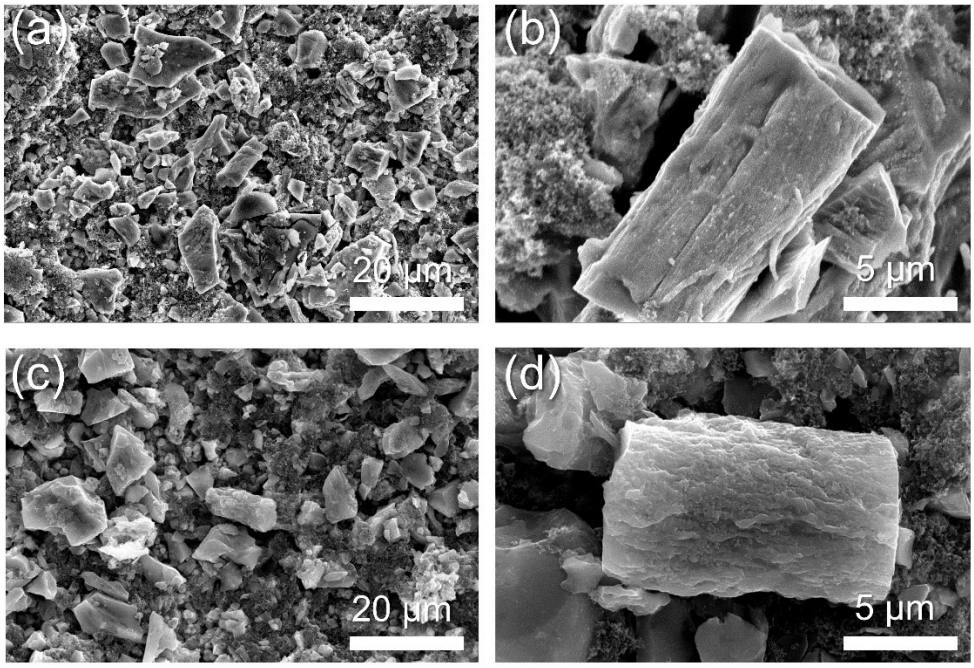

Figure S9. SEM images of N-C@$CoTe_2$@C electrode (a, b) before and (c, d) after 50 cycles at 0.5 A g^{-1}, respectively.

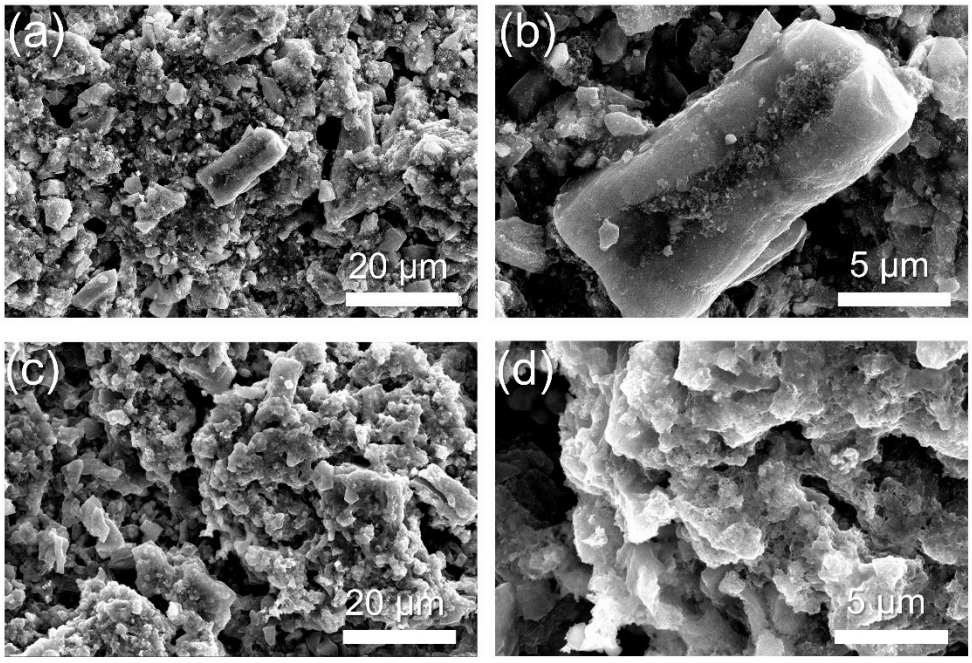

Figure S10. SEM images of $CoTe_2$@C electrode (a, b) before and (c, d) after 50 cycles at 0.5 A g^{-1}, respectively.

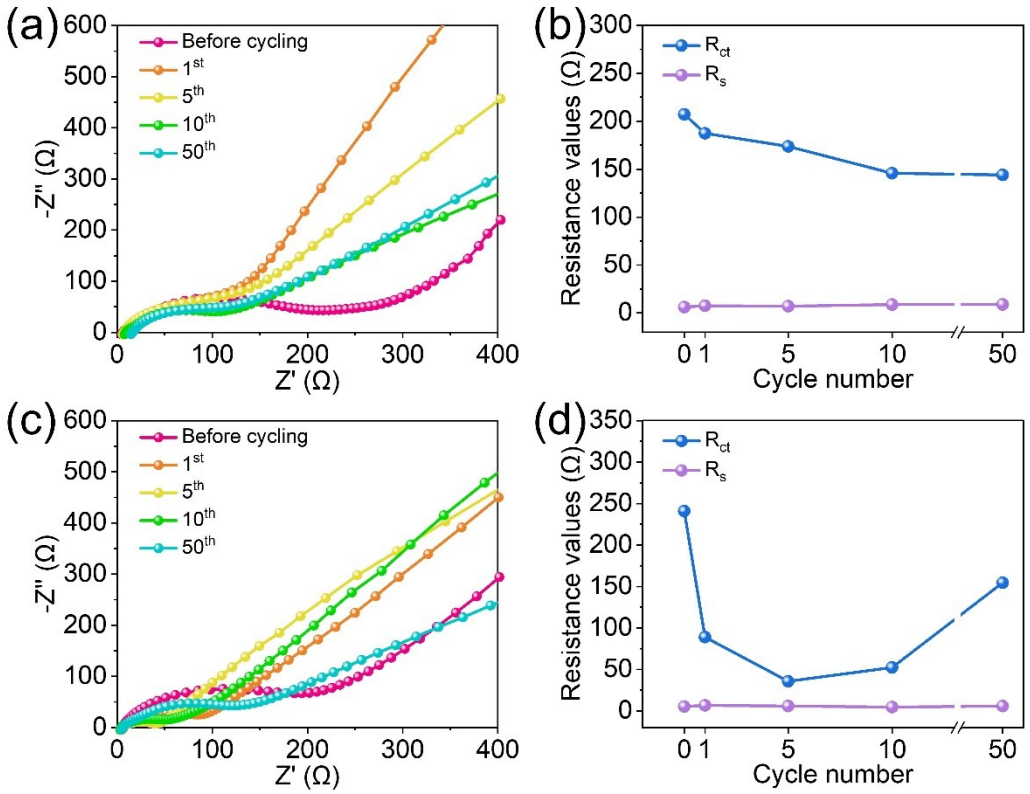

Figure S11. EIS curves and corresponding charge transfer resistance (R_{ct}) and internal resistance (R_s) results at different cycling states of (a, b) N-C@$CoTe_2$@C and (c, d) $CoTe_2$@C electrodes.

Figure R2a,b shows the EIS curves of the pristine N-C@$CoTe_2$@C electrode and its corresponding electrode after 1^{st}, 5^{th}, 10^{th}, and 50^{th} cycles. The diameters of the semicircle at high frequency decreases rapidly and remains stable after 10 cycles, which is attributed to the robust sandwich-type carbon framework that facilitates the formation of a stable SEI films. On the contrary, the continuous increase of the $CoTe_2$@C electrode due to the continuous pulverization of $CoTe_2$ particles that triggers the formation of fresh and thick SEI films. Furthermore, the EIS fitting results show that the charge transfer resistance (Rct) of the N-C@$CoTe_2$@C is more stable compared to that of $CoTe_2$@C, which further demonstrates the high stability and fast Na^+ kinetics of the C@$CoTe_2$@C electrode.

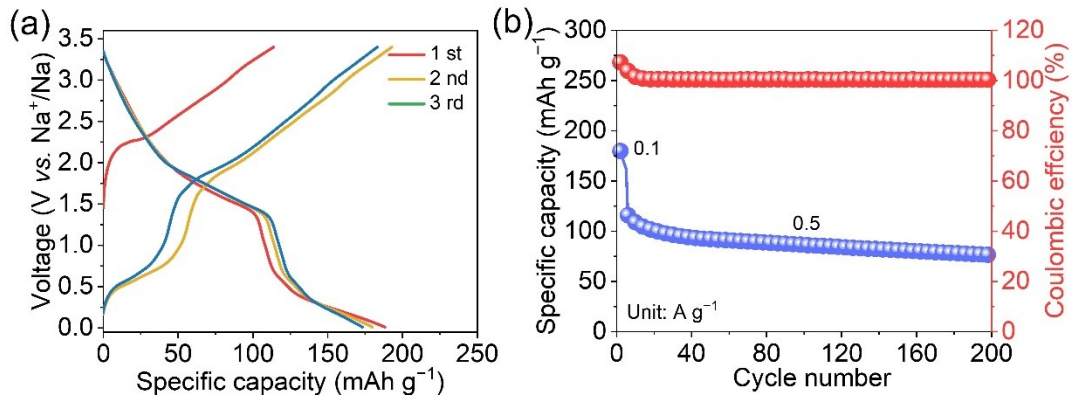

Figure S12. (a) Charge-discharge curves and (b) cycling performance at 0.5 A g^{-1} of $CoTe_2$@NMCNFs//P2-NaNMMT-4 full cells.

To reduce the capacity loss, the full cell was tested within the range of 0.01−3.4 V. As shown in **Figure S12a**, the charge/discharge curves of the N-C@$CoTe_2$@C//P2-NaNMMT full cell have an average discharge voltage of 2.1 V. Moreover, the full cell delivers a good reversible capacity of 76.3 mAh g^{-1}_{anode} after 200 cycles at 0.5 A g^{-1} with a Coulombic efficiency close to 100% (**Figure S12b**). The energy density of the $CoTe_2$@NMCNFs//P2-NaNMMT-4 full cell based on the total mass of anode.

Table. S1. Density of typical transition metal tellurides.

Materials	ZnTe	GeTe	CuTe	Sb_2Te_3	SnTe	$CoTe_2$
Density ($g\ cm^{-3}$)	6.34	6.14	7.1	6.5	6.48	7.92

Table. S2. Sodium storage cycling stability comparison of the N-C@$CoTe_2$@C electrode with other telluride-based anode materials in previous reports.

Materials	**Capacity (mAh g^{-1})**	**Cycle number**	**Ref.**
N-C@$CoTe_2$@C	198.5 mAh g^{-1} at 0.2 A g^{-1} 129.6 mAh g^{-1} at 0.5 A g^{-1} 85.7 mAh g^{-1} at 2.0 A g^{-1}	500 2000 3000	This work
Polyhedral $CoTe_2$-C	250 mAh g^{-1} at 0.35 A g^{-1}	200	S5
$CoTe_2$ nanorods/rGO	200 mAh g^{-1} at 0.1 A g^{-1}	200	S6
C@$Cu_{1.75}Te$	177.5 mAh g^{-1} at 0.1 A g^{-1}	500	S7
Sb_2Te_3/CNT	422 mAh g^{-1} at 0.1 A g^{-1}	300	S8
Sb_2Te_3/C	400 mAh g^{-1} at 0.1 A g^{-1} 360 mAh g^{-1} at 1.0 A g^{-1}	100 400	S9
Bi_2Te_3/G	319 mAh g^{-1} at 0.1 A g^{-1} 197 mAh g^{-1} at 2.0 A g^{-1}	100 500	S10
C@$MoTe_2$	286 mAh g^{-1} at 1.0 A g^{-1}	200	S11

References

1. B. Y. Kang, X. C. Chen, L. X. Zeng, F. Q. Luo, X. Y. Li, L. H. Xu, M.-Q. Yang, Q. H. Chen, M. D. Wei, Q. R. Qian, *J. Colloid Interface Sci*., 2020, **574**, 217−228.
2. Z. Y. Zhang, S. L. Wu, J. Y. Cheng, W. J. Zhang, *Energy Storage Mater*., 2018, **15***,* 65−74.
3. Z. L. Jian, Z. Y. Xing, C. Bommier, Z. F. Li, X. L. Ji, *Adv. Energy Mater*., 2016, **6** 1501874-1501878.
4. Y. Xu, C. L. Zhang, M. Zhou, Q. Fu, C. X. Zhao, M. H. Wu, Y. Lei, *Nat. Commun*., 2018, **9**, 1720-1730.
5. V. Ganesan, K.-H.Nam, C.-M. Park, *ACS Appl. Energy Mater*., 2020, **3**, 4877-4887.
6. Y. Ding, W. W. Wang, M. F. Bi, J. Y. Guo, Z. Fang, *Electrochim. Acta*., 2019, **313**, 331-340.
7. H. Yu, J. Yang, H. B. Geng, C. C. Li, *Nanotechnology*., 2017, **28***,* 145403-145410.
8. M. Ihsan-Ul-Haq, H. Huang, J. X. Wu, J. Cui, S. S. Yao, W. G. Chong, B. L. Huang, J.-K. Kim, Nano Energy., 2020, **71**, 104613.
9. Z. Yang, J. Y. Sun, Y. Z. Ni, Z. H. Zhao, J. M. Bao, S. Chen, *Energy Storage Mater*., 2017, **9**, 214-220.
10. D. D. Sun, G. J. Zhang, D. Li, S. T. Liu, X. L. Jia, J. S. Zhou, *Sustainable Energy Fuels*., 2019, **3**, 3163-3171.
11. J. S. Cho, H. S. Ju, J.-K. Lee, Y. C. Kang, *Nanoscale*., 2017, **9**, 1942–1950.